Proc. ESA Annual Meeting on Electrostatics 2010, Paper F4

The Assisted Corona Discharge: Multi-Electrode Configurations and the Effects on EHD Flows

Rakshit Tirumala and David B. Go[#]
Aerospace and Mechanical Engineering, University of Notre Dame
Notre Dame, IN, 46556 U.S.A.
[#]email: dgo@nd.edu

***Abstract* – Ionic winds formed by direct current corona discharges have recently gained increased popularity as a potential technology for the cooling of electronics. Scaling down ionic wind devices is particularly essential for mobile electronics so that the necessary operating voltages are at a reasonable level. However ionic wind-driven ducted blowers have yet to be widely adopted in small form factors (on the order of millimeters) because the formation and maintenance of stable coronas is difficult in such confined geometries. The present study proposes a multi-electrode configuration where two counter electrodes are utilized, and an assisted corona discharge is formed consisting of a primary corona discharge and a secondary discharge. Fundamental studies confirm that this assisted corona discharge is distinctly different than two independent corona discharges, and flow measurements demonstrate that it more efficiently generates ionic winds. The multi-electrode assisted discharge therefore offers a means to reduce operating voltages and address issues with the formation of a stable corona in narrow ducts.**

***Index Terms* – corona discharge, electrohydrodynamic flow, multiple electrodes, narrow channels, ionic wind, heat transfer**

I. INTRODUCTION

As electronics rapidly decrease in size, the design of novel small-scale heat transfer devices has garnered increased attention. Along with the minimization in size for portability, other issues like low acoustic signature and reliability also feature as significant factors in the search for new technologies to replace the traditional fan as the primary cooling apparatus. Studied for over 50 years in the field of electrostatic precipitation, for the past two decades, the corona discharge-driven ionic wind, or more generally electrohydrodynamic (EHD) flow, is a technology that has emerged as one of the popular solutions to the electronics cooling challenge. As both a mechanism for spot cooling [1-3] as well as for the design of blowers [4-7], the ionic wind produced by

corona discharges is an attractive solution because of its many advantages—the absence of moving parts, size, weight, low acoustic signature, and ease of operation.

Though ionic winds can be produced by other gas discharges, dielectric barrier discharges being a commonly used one, corona discharges offer the advantage of easy operation in direct current (D.C.) mode at atmospheric pressures giving rise to a steady current. Corona discharges occur between a sharp electrode (called a corona source), typically a pin or a wire, and a blunt electrode (called a counter electrode) like a plate or a cylinder. Because corona discharges are a partial breakdown of the air gap, they are highly dependent on the inhomogeneity of the electric field between the sharp and blunt electrodes. Corona discharges, and as an extension, ionic winds, can be obtained in both positive and negative polarity depending on which way the potential difference is applied on the electrodes. A positive corona discharge generates ions near the sharp electrode which, driven by the electric field, drift towards the counter electrode. Along the way, their collisions with neutral air molecules transfer momentum, generating a bulk flow—an ionic wind (also called a corona or electric wind).

Gas pumps utilizing corona winds as the flow driving mechanism have been developed over the years [5-8]. Various electrode geometries have been used in these designs, the most popular being pin to plate, wire to plate, wire to mesh, and wire to cylinder configurations. However, these ionic wind blowers are on a scale that is still unsuitable for adaptation as cooling applications in small form-factor electronics. These gas pumps have cross section diameters and channel heights typically on the order of 10 mm. Portable electronics require the blowers to be on a significantly smaller scale, with the desired channel heights on the order of 2 mm. There has been little development in the miniaturization of the ionic wind blowers to such small scales.

Takeuchi and Yasuoka [9] carried out ionic wind experiments in ducts of varying diameters. They observed that obtaining a stable corona discharge becomes increasingly difficult as the cross section of the duct is reduced and becomes nearly impossible for diameters less than 5 mm. This has also been confirmed in the course of the experiments that led to this present article wherein it was observed that the discharge transitioned to a spark without the formation of a stable corona. One possible reason put forth as an explanation for this observation is that the dielectric channel walls constrain the electric field lines to be tangential along the dielectric surfaces and hence confine the electric field lines to flow within the channel. As the channel height is reduced, the field lines become almost parallel and the requirement of a non-uniform field near the source is not fulfilled. As such, the discharge takes on the characteristics of a uniform field glow discharge, which is typically not stable at atmospheric pressure. While the above explanation is speculative, the fact that a traditional corona discharge is hard to maintain in small channels motivates the exploration of novel design configurations.

Another issue important in the application of ionic wind blowers to portable electronics is the minimization of the potential used to drive the flow. Safety and power source requirements force the applied potential to be minimized with a final goal below 2000V. This restricts the flow rate that can be obtained using the corona discharge since

the flow velocity is proportional to the corona current, which itself increases with increased potential difference. Also, the minimization of the applied voltage limits the gap between the electrodes since the corona onset potential increases as the gap is increased. Reducing the electrode gap has a negative impact on the flow rate since the drift region is reduced in length, implying that the ions undergo fewer momentum-transfer collisions with the bulk flow.

The present article proposes a multi-electrode configuration to tackle the above issues. While corona discharges have previously been carried out in multiple electrode configurations, both as multiple sources and multiple counter electrodes, they have typically maintained all the electrodes at the same potential and operate in symmetric configurations [8]. Very few [10-11] have carried out any research on configurations in which the various electrodes are each maintained at their own potential. Recently Bendaoud et al. [12] used a similar concept to address the issue for electrostatic precipitation. In this work, fundamental experiments have been conducted to characterize and understand the physics of the discharge in multi-electrode configurations. Preliminary flow measurements suggest that this multi-electrode approach is inherently more efficient that the traditional two-electrode corona discharge.

II. THE MULTI-ELECTRODE CORONA DISCHARGE: METHOD AND EXPERIMENTAL APPARATUS

A basic schematic for the multiple-electrode discharge is shown in Fig.1. Note that this figure is only an example and various other configurations have also been studied. For the purposes of the present article, only the work carried out between a wire and two counter electrodes are discussed. It should be mentioned however, that the results shown here follow more or less similar trends with the use of a pin as the corona source.

In a traditional two-electrode configuration, the positive ions are driven by the electric field from the source towards the counter electrode. The conceptual impetus for the three-electrode arrangement is to apply an additional electric field downstream of the ion source to pull the ions away from the primary counter electrode (labeled as electrode-2) and drive them towards electrode-3. In principle, the distance between the primary electrode (2) and the corona source (1) could be reduced without reducing the flow rate, allowing a reduction in both the onset and operating potential. Essentially, in this configuration electrode-2 acts as a gate electrode whereas electrode-3 acts to drive the ionic wind as illustrated in Fig. 2. Jewell-Larsen [13] describes a similar concept using an enhancement electrode and a collector electrode. Recently, Colas et al. [14] have used the same concept of multi-electrode configurations and claim to have decoupled the ionization and acceleration processes. However, it should be mentioned that the length scales and potentials used in this study were much larger than what is desired for small-

scale ionic wind blowers, operating at duct heights of about 10 mm and potentials of about 20kV.

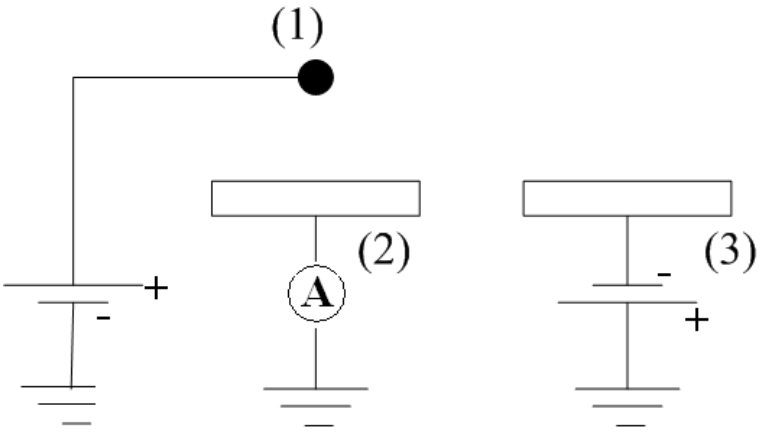

Fig. 1. Schematic of a typical 3-electrode corona discharge setup

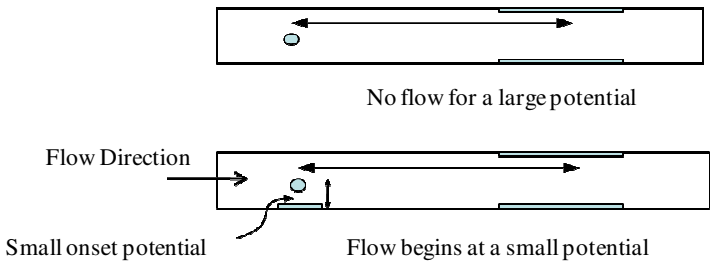

Fig. 2. Example schematic showing the application of the multi-electrode corona discharge in an EHD-driven channel flow. In the top figure, the gap between the corona source and downstream electrodes is too large to initiate a corona discharge or ionic wind for a given potential. However, in the bottom figure, by using a gate electrode that is closer to the corona source, a discharge is ignited at a lower applied potential and the flow is driven by the downstream electrodes.

Two configurations were studied to analyze the discharge behavior in a 3-electrode configuration as shown in Figs. 3a and 3b. Henceforth, the setups shall be referred to as Configurations-A and -B respectively. Both configurations used a 50 μm diameter tungsten wire as the corona source. Configuration-A in Fig. 3a shows a 3-electrode configuration built into a channel with a cross section of 40 × 4 mm and a length of 100 mm. The wire was strung along the entire width of the channel, and the

counter electrodes were pieces of 5 mm wide copper tape along the entire channel width. The gap between the wire and electrode-2 was 2 mm and the gap between the two counter electrodes was 3 mm. Flow was measured using an Extech Instruments handheld hot wire thermo-anemometer at the exit of the channel. Configuration-B in Fig. 3b consisted of the corona wire strung between two copper counter electrodes positioned on each side in open air. Both the wire and the counter electrodes were 40 mm in width. The distance from the wire to electrode-2 was maintained constant at d_0 = 4.2 mm and the distance to electrode-3, d, was adjusted using a motorized linear stage. In both configurations, a positive potential ($\Phi_{wire} > 0$) was applied to the corona wire using a Bertan-225 D.C. power supply. Currents were either measured off the counter electrodes (-2 and -3) sequentially using a Keithley 6485 picoammeter or sometimes simultaneously (as noted below) using a second Keithley 6487 picoammeter. In most studies, electrode-2 was maintained at a ground potential ($\Phi_2 = 0$ V) while a negative potential ($\Phi_3 < 0$) was applied to electrode-3 using a second power supply (UltraVolt HV Rack).

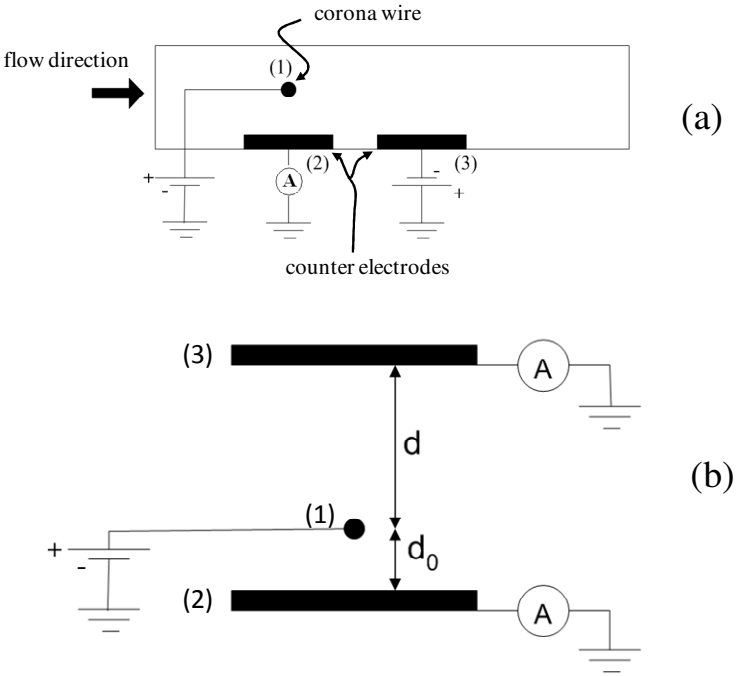

Fig. 3 Schematics of (a) Configuration-A (channel flow) and (b) Configuration-B where d_0 was fixed and d was adjustable.

III. RESULTS

I. Configuration-A: Electrical Discharge Characteristics

In Configuration-A, a typical study consisted of increasing the applied potential to the corona wire (Φ_{wire}) from onset to spark-over while sequentially measuring the current through electrodes-2 and -3 (I_2 and I_3, respectively). Electrode-2 was maintained at ground potential (Φ_2 = 0 V) for all experiments, and three applied potential conditions were used for electrode-3: floating potential (open), Φ_3 = -1000 V, and Φ_3 = -2000 V. In this first condition, there is no significant electric field between electrodes-2 and -3 and the corona discharge is a standard two-electrode discharge from the corona wire to electrode-2. In the latter conditions, an electric field was imposed between electrodes-2 and -3 to create a multi-electrode corona discharge. As a matter of comparison, in a fourth case, the applied potential on electrode-3 was maintained at ground (Φ_3 = 0 V) and electrode-2 was under a floating potential. This represents the case where a standard two-electrode corona discharge is generated between the corona wire and electrode-3. Fig. 4 shows the current measured through electrode-2 (Fig. 4a) and electrode-3 (Fig. 4b) for the various cases.

As can be seen in Fig. 4a, the current through the primary counter electrode (I_2) remains largely unchanged regardless of the condition on electrode-3. Neither the presence of electrode-3 nor the potential applied on it appears to have any noticeable impact on the current through electrode-2. That is, regardless of Φ_3, I_2 always resembles a standard two-electrode discharge between the corona wire and electrode-2. Additionally, for all conditions on electrode-3, the onset potential ($\Phi_{wire,o}$) for electrode-2 was approximately 2900 V.

Fig. 4b shows the current through electrode-3, I_3, for the conditions where Φ_3 = -1000 V and Φ_3 = -2000 V. For the special case when Φ_3 = 0 V and electrode-2 was floating, corona never onset up to Φ_{wire} = 6200 V, at which point it sparked, implying a standard two-electrode corona discharge was not possible between the corona wire and electrode-3 for this geometry. As is apparent, when there is an electric field applied between electrodes-2 and -3, there is appreciable current flow through both electrodes even below Φ_{wire} = 6200 V. In fact, when $\Phi_3 < 0$, the current to electrode-3 initiates at ~2900 V, which is consistent with $\Phi_{wire,o}$ for electrode-2. This observation suggests that when a multi-electrode configuration is used, the current generated to electrode-3 is not a corona discharge between the corona wire and electrode-3; at least not in the traditional sense. As noted above, in the multi-electrode configuration, the current to electrode-2 does behave like a standard corona discharge. However, by comparing Figs. 4a and 4b, it can be seen that the increase in I_3 does not correspond to a decrease in I_2. Therefore, in a multi-electrode configuration a standard corona discharge is generated to electrode-2 and a secondary discharge is generated to electrode-3. This multi-electrode discharge consisting of a standard and secondary discharge can be called an *assisted corona discharge* because the presence of electrode-2 is necessary to ignite I_3 at ~2900 V. Further, because I_3 does not impact I_2, the overall current from the discharge localized

around the wire increases in the multi-electrode assisted corona discharge. In this particular configuration-A, I_3 was roughly an order of magnitude lower than I_2. However, this current ratio can be improved depending on the geometry as discussed in the fundamental studies using configuration-B.

II. Configuration-A: Flow Characteristics

Flow measurements were conducted at the exit of the duct in Configuration-A using the hand-held velocimeter. Fig. 5a plots the measured exit flow velocity (u_{exit}) against the potential on the corona wire. Second order polynomial curves have been fit to the data points to illustrate the trends clearly but these should not be taken as having distinct physical meaning. There are two observations that can be made. First, when Φ_3 is left floating, the velocity generated is due entirely to the two-electrode corona discharge between the wire and electrode-2. The plot in Fig. 5a shows that this velocity stagnates at about 0.2 m/s. This is not surprising since the two-electrode configuration has the electrode directly beneath the corona wire and the ions have minimal drift in the flow direction. However, when $\Phi_3 < 0$, the multi-electrode assisted discharge is active and this results in an increased flow rate. This observation can be attributed to the fact that the increased current in a 3-electrode discharge has a longer drift region between the wire and electrode-3, where it is more effective in transferring momentum to the bulk flow. In additional studies not presented here, electrode-2 was placed slightly downstream of the corona source and the velocity continuously increased with Φ_{wire}. However, even in that configuration, the application of $\Phi_3 < 0$ still resulted in an assisted discharge and increased exit velocity.

The second observation is that the flow velocity increases as Φ_3 decreases (increasing the potential difference $\Phi_{wire} - \Phi_3$), which is also consistent with the current observations in Fig. 4b. While the application of a negative potential on electrode-3 implies that the total potential difference used is higher, it should be noted that in narrow channels of heights less than 4 mm, it is difficult to obtain a stable corona discharge with the collecting electrode downstream of the wire. Thus, the primary collecting electrode-2 should be placed as close to the wire as possible, which will reduce its contribution to the flow. The multi-electrode configuration has the potential to address the issue with the optimized design of the electrodes.

Fig. 5b plots electrical power consumption against the exit flow velocity generated. For the power consumption in the multi-electrode configuration, Kirchoff's law was used to calculate the power as

$$P = (\Phi_{wire} - \Phi_2) I_2 + (\Phi_{wire} - \Phi_3) I_3 \,. \qquad (1)$$

The multi-electrode assisted discharge is clearly seen to be more efficient because less power is consumed to generate a given amount of flow, and it continues to gain

efficiency as Φ_3 decreases increasing $\Phi_{wire} - \Phi_3$. For instance, Φ_3 = -1000 V requires nearly twice as much electrical power to obtain a u_{exit} = 0.5 m/s as Φ_3 = -2000 V does. The gain in efficiency can be attributed to the larger drift region available to the ions.

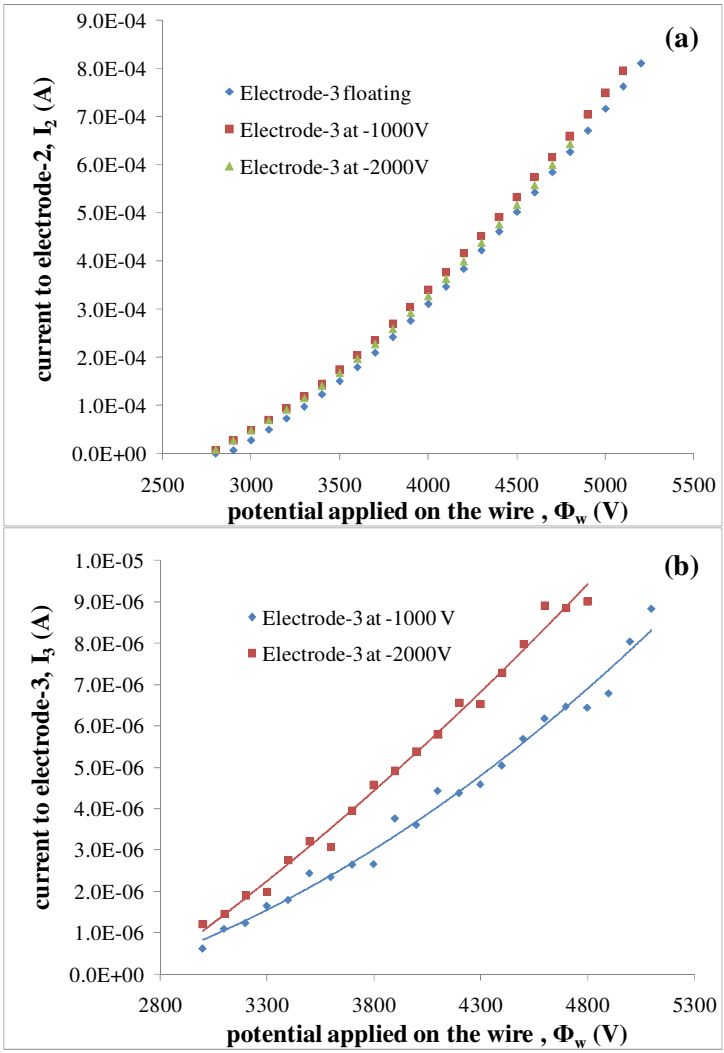

Fig. 4 The current as a function of the potential applied to the corona wire (Φwire) as measured through (a) electrode-2, *I*2 and (b) electrode-3, *I*3.

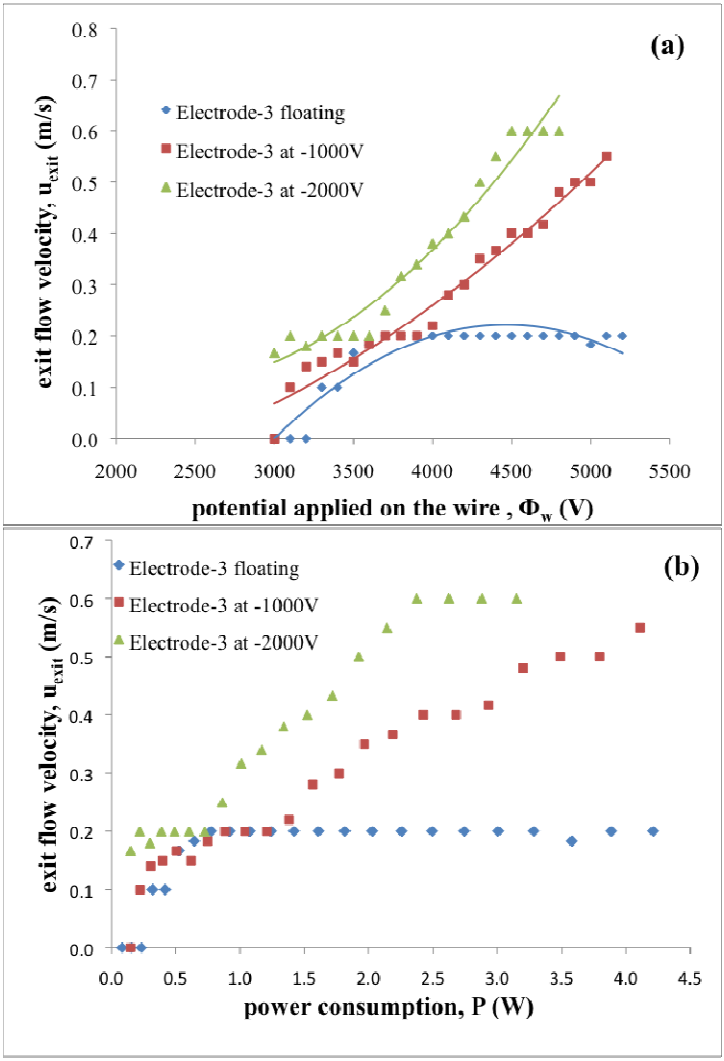

Fig. 5 Plot of the exit flow velocity (u_{exit}) as a function of (a) the potential applied to the corona wire (Φ_{wire}) and (b) the power consumption (P).

III. Configuration-B: Electrical Discharge Characteristics

To understand the physical mechanism behind the multi-electrode assisted discharge, fundamental studies were performed on the simpler setup shown as Configuration-B. This configuration was studied for its simplicity in theoretical analysis. For a 2-electrode wire-plate configuration, the theoretical current-voltage relationship is given by Townsend's discharge equation

$$I = \frac{k}{d^2\left(\ln\left(\frac{2d}{r}\right)\right)^2}\Phi(\Phi - \Phi_o), \qquad (2)$$

where d is the distance between the wire and the plate, r is the radius of the wire, Φ is the applied potential and Φ_o is the onset potential. k is a constant that depends on the mobility of ions in the flow medium (in this case air) and the permittivity of free space. It also varies slightly based on the atmospheric conditions and cleanliness of the electrodes. It should be noted that Eq. 2 has two main components—a geometric dependence on the gap distance and wire radius, and a potential component.

To obtain the geometric and potential dependences of the discharge in a 3-electrode configuration, the experiments were carried out in two separate sets. In one, electrodes -2 and -3 were both grounded, the distance to electrode-3 (d) was varied, and currents I_2 and I_3 were measured simultaneously with two picoammeters. The results of this experiment described the geometric behavior of the discharge. In the second set of experiments, the distances d_0 and d were maintained constant, electrode-2 was grounded, and a negative potential was applied on electrode-3 (analogous to Configuration-A). I_2 and I_3 were again measured simultaneously. This characterizes the multi-electrode assisted discharge's behavior based on the applied potentials and resulting electric fields.

Figs. 6 and 7 show the results of the geometric behavior in the first set of experiments where electrode-2 was fixed at a constant distance of d_0 = 4.22 mm from the wire. The distance d from electrode-3 to the wire was varied from 4.2 mm to 12.6 mm in steps of 2.1 mm (*i.e.*, the gap d/d_0 ratio was increased as 1, 1.5, 2, 2.5, 3, and 3.5). Fig. 6a shows the current through electrode-3 (I_3) where Φ_3 = 0 V and electrode-2 was left floating. This represents a standard two-electrode corona discharge between the wire and electrode-3 for varying gap distances, and as expected, the onset voltage $\Phi_{wire,o}$ increases as d increases. In Fig. 6b, $\Phi_2 = \Phi_3$ = 0 V, and I_2 is largely unaffected by the presence of electrode-3 (though there is a slight decrease), regardless of its proximity to the corona wire—a result consistent with Fig. 4a for Configuration-A. As shown in Fig. 7a for $\Phi_2 = \Phi_3$ = 0 V, there is significant current to electrode-3 at all d, and I_3 decreases as d increases, which is expected. However, in comparing Fig. 6a and Fig. 7a, it is apparent that the presence of electrode-2 at Φ_2 = 0 V ignites a discharge to electrode-3 consistently at Φ_{wire} = 3100 V *regardless of the gap distance d*, and this is much lower than the $\Phi_{wire,o}$ required if electrode-2 was absent as shown in Fig. 6a. This confirms the similar

observation in Configuration-A—that it is possible to ignite a multi-electrode assisted discharge at applied potential. Though it is not presented in these figures for conciseness, it should be noted that I_3 in Fig. 7a is much greater than the slight loss in I_2 observed in Fig. 4b, *i.e.*, the total current is increased as previously suggested with Configuration-A.

One special case occurs in Fig. 7a when $d = d_0 = 4.2$ mm, and the gap distance is symmetric. In this case, two independent coronas are formed—one between the wire and electrode-2 and one between the wire and electrode-3. This was confirmed by plotting the $d = d_0 = 4.2$ mm on the same plot as Fig. 6b (not shown for brevity). However, this observation raised the question as to whether the assisted discharge as observed in Configuration-A is truly a combination of a corona to electrode-2 and a secondary discharge to electrode-3, or the superposition of two independent corona discharges—one to electrode-2 and one to electrode-3. To explore this, Fig. 7b plots the ratio of I_3 at a distance d from Fig 7a (the multi-electrode assisted discharge) against its value at $d = d_0 = 4.2$ mm (when it is an independent corona). In principle, if $I_3(d)$ is an independent corona for all d, then $I_3(d)$ should follow Eq. 2. Further, if the ratio of currents is considered from Eq. 2 at any two distances, one obtains

$$\frac{I_3(d)}{I_3(d_0)} = \left(\frac{d_0 \ln\left(\frac{2d_0}{r}\right)}{d \ln\left(\frac{2d}{r}\right)} \right)^2, \qquad (3)$$

Note that this ratio assumes that Φ_{wire} and Φ_o are the same regardless of d, but this has been confirmed in Fig. 7a. Therefore, if the current to electrode-3 is its own corona, this ratio should be a constant for a given distance d—that is the ratio is entirely geometry dependant. However, as shown in Fig. 7b, initially, soon after onset, the measured ratio does not follow the theoretically predicted ratio, but asymptotes to it as Φ_{wire} increases. Therefore, this suggests there are two regimes—initially I_3 is due to an assisted discharge, but at some point it transitions to its own, independent corona discharge. It should be noted that all the studies in Configuration-A operated in this initial regime. It should also be noted that the potential at which the discharge asymptotes is not the same as the onset potential for electrode-3 that is obtained from Fig. 6a. Future studies are planned to fully characterize and understand these two regimes and how the discharge transitions between them.

Fig. 8 studies the effect of a negative potential ($\Phi_3 < 0$ V) on electrode-3 on the discharge when it is maintained at a fixed distance $d > d_0$. Since this negative potential might onset corona earlier on electrode-3, the distance to electrode-3 was set at $d = 14.7$ mm to ensure that it operated in the assisted discharge regime without transitioning to an independent corona discharge. The plot shows that I_3 expectedly increases as Φ_3 becomes more negative. It was also observed, though not shown, that the application and magnitude of Φ_3 has little impact on I_2 – consistent with all the other results presented

here. It has not yet been determined whether the discharge follows the quadratic relationship of the Townsend's equation and work is ongoing to model the characteristics both theoretically and computationally.

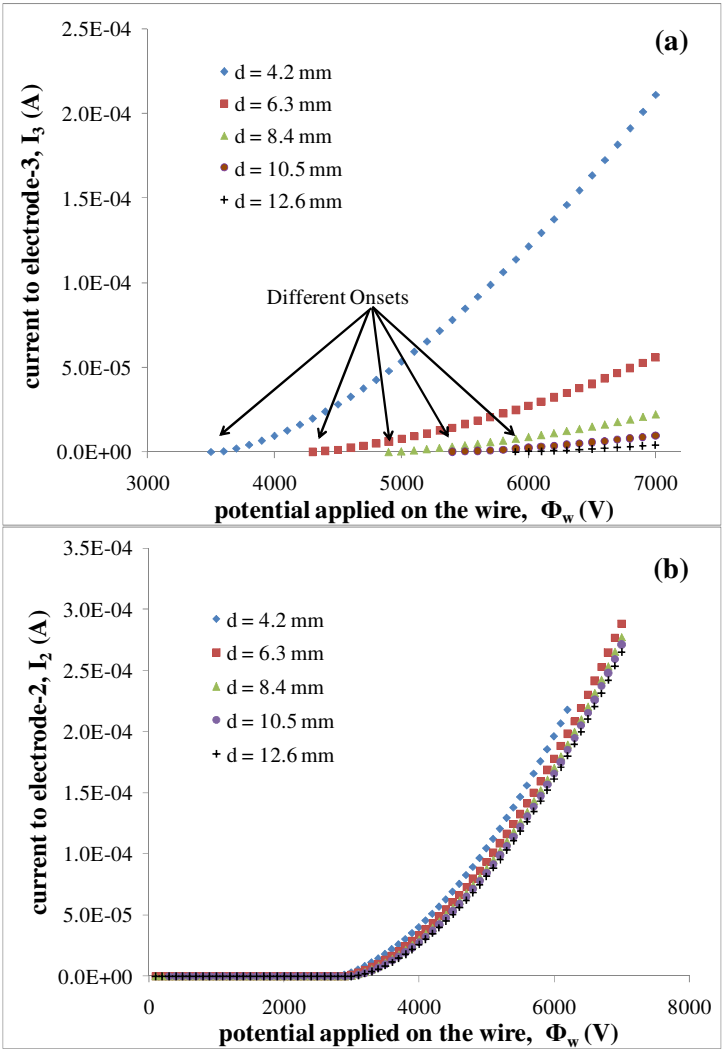

Fig. 6 The current as a function of the potential applied to the corona wire (Φ_{wire}) as measured through (a) electrode-3 (I_3) where $\Phi_3 = 0$ V and Φ_2 is floating, (b) electrode-2 (I_2) for different distances d of electrode-3 where $\Phi_2 = \Phi_3 = 0$ V

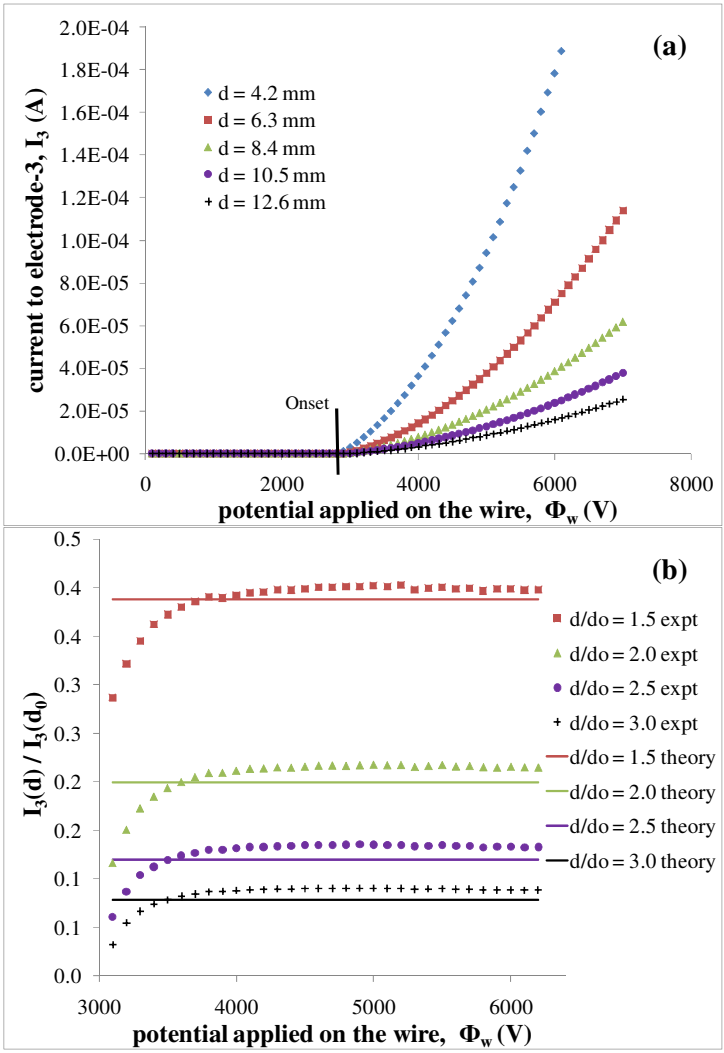

Fig. 7 The current as a function of the potential applied to the corona wire (Φ_{wire}) as measured through (a) electrode-3 (I_3) for different distances d of electrode-3 where $\Phi_2 = \Phi_3 = 0$ V. (b) The measured and theoretical ratio of I_3 values as a function of the potential applied to the corona wire (Φ_{wire}).

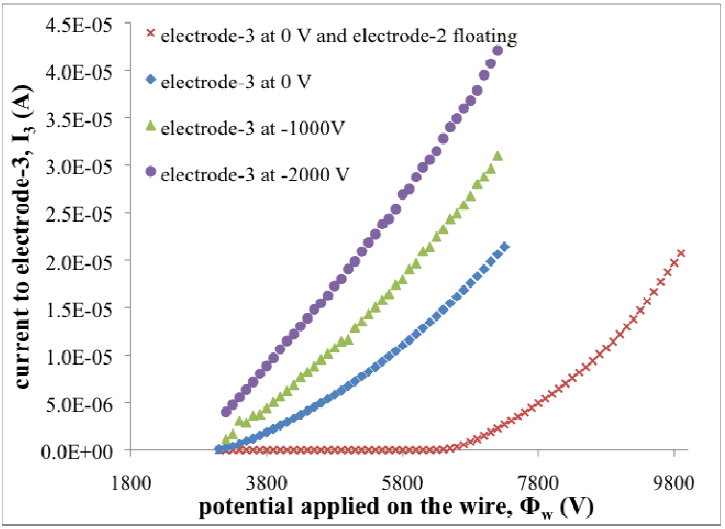

Fig. 8. Current through electrode-3 (I_3) as a function of the potential applied to the corona wire (Φ_{wire}) for different values of Φ_3. In all cases, d = 14.7 mm and Φ_2 = 0 V.

IV. DISCUSSION AND CONCLUSIONS

In the above work, a multi-electrode corona discharge configuration has been presented to generate flows in narrow channels at low voltages. Electrical measurements demonstrate that the multi-electrode configuration generates an assisted corona discharge, whereby a standard corona discharge is generated to the near electrode and a non-corona secondary discharge is generated to the far electrode. Further, it has been demonstrated that at some applied potential to the wire (depending on the geometry and configuration), the assisted discharge transitions to two independent corona discharges to each collecting electrode. When configured in a channel, the multi-electrode corona discharge not only increases the overall flow rate, but does so in an efficient manner. These studies suggest that multi-electrode assisted discharges can be used to overcome challenges to implementing ionic winds in small-form factor electronic devices, where a primary counter electrode is used as a gate electrode but a secondary collecting electrode is used to drive the flow. This approach provides an avenue to reduce operating voltages, reduce the onset potential, and enable low power performance. Further ongoing studies aim to explain the physical mechanism of the assisted discharge formation and optimization of the assisted discharge driven EHD gas pump.

ACKNOWLEDGEMENTS

The authors would like to acknowledge technical discussions and funding support from Intel Corporation.

REFERENCES

[1] D. B. Go, S. V. Garimella, T. S. Fisher, R. K. Mongia, "Ionic winds for locally enhanced cooling," *J. Appl. Phys.*, vol. 102, art. no. 053302, 2007.

[2] D. B. Go, R. A. Maturana, T. S. Fisher, S. V. Garimella, "Enhancement of external forced convection by ionic wind," *Int. J. Heat Mass Transfer*, vol. 51, pp. 6047-6053, 2008.

[3] C. P. Hsu, N. E. Jewell-Larsen, C. Sticht, I. A. Krichtafovitch, A. V. Mamishev, "Heat transfer enhancement measurement for microfabricated electrostatic fluid accelerators," *Proc. Of 24th Annual IEEE Semiconductor Thermal Measurement and Management Symposium*, Semi-Therm, Santa Clara, CA, pp. 32-37, 2008.

[4] N. E. Jewell-Larsen, H. Ran, Y. Zhang, M. Schwiebert and K. A. Honer, "Electrohydrodynamically cooled laptop", *Proc. Of 25th Annual IEEE Semiconductor Thermal Measurement and Management Symposium*, Semi-Therm, Santa Clara, CA, pp. 261-266, 2009.

[5] B. Komeili, J. S. Chang, G. D. Harvel, C. Y. Ching, D. Brocilo, "Flow characteristics of wire-rod type electrohydrodynamic gas pump under negative corona operations", *J. Electrostat.*, vol. 66, pp. 342-353, 2008.

[6] M. Rickard, D. Dunn-Rankin, F. Weinberg, F. Carleton, "Maximizing ion-driven gas flows," *J. Electrostat.*, vol. 64, pp. 368-376, 2006.

[7] D. Schlitz, V. Singhal, "An electro-aerodynamic solid-state fan and cooling system", *Proc. Of 24th Annual IEEE Semiconductor Thermal Measurement and Management Symposium*, Semi-Therm, Santa Clara, CA, pp. 46-49, 2008.

[8] N. E. Jewell-Larsen, I. A. Krichtafovitch, A. V. Mamishev, "Design and optimization of electrostatic fluid accelerators", *IEEE Trans. Dielec. El. In.*, vol. 13, No. 1, 2006.

[9] N. Takeuchi, K. Yasuoka, "Gas discharge induced electrohydrodynamic flow in narrow channels," presented at the *Electrostatics Joint Conference*, Boston, MA, 2009.

[10] G. F. Ferreira, D. L. Chinaglia, J. A. Giacometti, O. N. Oliveira Jr., "Corona triode current-voltage characteristics: on effects possible caused by the electronic component," *J. Phys. D: Appl. Phys.*, vol. 26, No.4, 1993.

[11] X. Deng and K. Adamiak, "The electric corona discharge in a triode system," *IEEE Trans. Ind. Appl.,* vol. 35, No. 4, 1999.

[12] A. Bendaoud, A. Tilmantine, K. Medles, M. Younes, O. Blejan , L. Dascalescu, "Experimental Study of corona discharge generated in a modified wire-plate

electrode configuration for electrostatics process applications", *IEEE Trans. Ind. Appl.,* vol. 46, No. 2, 2010.

[13] N.E. Jewell-Larsen, "Optimization and miniaturization of electrostatic air pumps for thermal management", M.S. Thesis, Dept. of Elec. Eng., Univ. of Washington, Seattle, WA, 2004.

[14] D. Colas, A. Ferret, I. Sciacca, D.Z. Pai, D.A. Lacoste, C.O. Laux, "Novel electrode configuration for ionic wind generation in air at atmospheric pressure", presented at the 3rd European Conference for Aerospace Sciences (EUCASS), Versailles, 2009.